

# HOW TO BUILD A PRE-TRAINED MULTIMODAL MODEL FOR SIMULTANEOUSLY CHATTING AND DECISION-MAKING?

**Anonymous authors**

Paper under double-blind review

## ABSTRACT

Existing large pre-trained models typically map text input to text output in an end-to-end manner, such as ChatGPT, or map a segment of text input to a hierarchy of action decisions, such as OpenVLA. However, humans can simultaneously generate text and actions when receiving specific input signals. For example, a driver can make precise driving decisions while conversing with a friend in the passenger seat. Motivated by this observation, we consider the following question in this work: is it possible to construct a pre-trained model that can provide both language interaction and precise decision-making capabilities in dynamic open scenarios. We provide a definitive answer to this question by developing a new model architecture termed Visual Language Action model for Chatting and Decision Making (VLA4CD), and further demonstrating its performance in challenging autonomous driving tasks. We build VLA4CD on the basis of transformer-based LLM architecture. Specifically, we leverage LoRA to fine-tune a pre-trained LLM with data of multiple modalities covering language, visual, and action. Unlike the existing LoRA operations used for LLM fine-tuning, we have designed new computational modules and training cost functions for VLA4CD. These designs enable VLA4CD to provide continuous-valued action decisions while outputting text responses. In contrast, existing LLMs can only output text responses, and current VLA models can only output action decisions. Moreover, these VLA models handle action data by discretizing and then tokenizing the discretized actions, a method unsuitable for complex decision-making tasks involving high-dimensional continuous-valued action vectors, such as autonomous driving. The extensive experimental results on the closed-loop autonomous driving platform CARLA validate that: (1) the model construction method we proposed is effective; (2) compared to the state-of-the-art VLA model, VLA4CD can provide more accurate real-time decision-making while retaining the text interaction capability inherent to LLMs.

## 1 INTRODUCTION

Since the emergence of ChatGPT, large-scale pre-trained models, represented by large language models (LLMs), have garnered increasing attention. LLMs are trained on vast amounts of text and code data on the internet, encoding a significant amount of general knowledge about the real world. This equips them with better generalization capabilities compared to traditional AI models, such as in-context learning abilities and certain reasoning capabilities (through techniques such as chain-of-thought (Wei et al., 2022)). A development trend in the field of large-scale pre-trained models is that their application domains are expanding from tasks like dialogue and text generation to decision-making tasks in the open physical world.

How to build large-scale pre-trained models for decision-making tasks in the open physical world? Currently, there are three major approaches. An approach is to serialize the decision-making process and then train a sequence model, such as the decision transformer (Chen et al., 2021), in the same way as processing text. This method relies on the construction of large-scale high-quality decision-making datasets. The second approach involves adopting a hierarchical modular system design, where the pre-trained LLM provides high-level planning, such as breaking down the target

task into a series of subtasks and then completing each subtask by calling tools or small models aimed at the subtasks (Chen et al., 2024; Carta et al., 2023; Hu et al., 2024; Zhou et al., 2024). This approach requires manual pre-design of system modularization and the establishment of interfaces between modules. Additionally, after the model is deployed, in addition to the latency caused by LLM inference, it also introduces the working latency of other modules, making it unsuitable for decision-making scenarios with high-time requirements. The last approach is to train a multimodal visual language action model (VLA) based on LLM (Padalkar et al., 2023; Kim et al., 2024). Unlike the hierarchical modular method, the VLA model can provide end-to-end decision generation, eliminating the need for manual module design and interface design between modules.

To the best of our knowledge, existing LLM or VLA models, given an input signal (a piece of text prompt, an image, or a video), produce outputs that are single-modal (a piece of text or an action decision). However, we know that for us humans, we can simultaneously generate text and actions when receiving specific input signals. For example, a driver can make precise driving decisions while conversing with a friend in the passenger seat. Inspired by the above observations, we attempt to answer the following question in this paper:

***Is it possible to develop a pre-trained model that can provide both action decision-making and text interaction capabilities in an end-to-end manner?***

We provide a definitive answer to it by developing a new model architecture termed Visual Language Action model for Chatting and Decision Making (VLA4CD), and further demonstrating its performance in challenging autonomous driving tasks. Like existing VLA models, VLA4CD is a multimodal pre-trained large model developed based on the transformer architecture. However, it has significant differences from current VLAs (such as RT-X (Brohan et al., 2022; 2023)):

- The operational mechanism of VLA involves executing serialized decisions after receiving text instructions, without generating text data during the decision-making process. In contrast, VLA4CD allows for the synchronous generation of text data during real-time decision-making.
- Current VLA models typically handle action data by discretizing it and then tokenizing the discrete values. This approach is not suitable for complex decision-making scenarios such as autonomous driving, where actions are high-dimensional continuous value vectors. Our VLA4CD processes actions directly as continuous values, eliminating the need for discretization and making it more suitable for such scenarios.

In summary, the *main contributions* of this work are as follows.

- We propose a new problem setting: how to synthesize the capabilities of LLM and VLA using a single model to achieve end-to-end simultaneous action decision-making and chatting with people.
- We present a solution to the aforementioned problem. Specifically, we propose a method for constructing VLA4CD based on pre-trained LLM and have validated the effectiveness and superiority of this method through extensive closed-loop autonomous driving experiments on CARLA (Dosovitskiy et al., 2017). The experimental results show that the resulting VLA4CD model not only outputs more accurate real-time action decisions compared to the SOTA models but also perfectly retains real-time text-based dialogue functionality. Our method combines several experimentally validated ideas: (1) a computational module and cost function term for generating continuous action values; (2) an image reconstruction loss term added in the training cost function to ensure the exploitation of rich information from the visual modality data during text generation and decision-making processes; (3) a label smoothing strategy to maintain dialogue capabilities and enhance decision-making.
- We will open source our model, code, and dataset after the reviewing process.

## 2 RELATED WORK

### 2.1 LLMs FOR DECISION-MAKING

Since the publication of (Brown et al., 2020), generative Pre-trained Transformer (GPT) has become the most popular training paradigm for building LLMs. LLMs represented by GPT-3.5 and

GPT-4 exhibit significantly enhanced zero-shot generalization and reasoning capabilities compared to previous language models (OpenAI, 2023). The release of the open-source LLaMA series models (Touvron et al., 2023a;b) has accelerated the development of LLMs. In (Wei et al., 2022), a general technique to enhance LLM reasoning capabilities, known as chain-of-thought, was proposed. The work in (Yao et al., 2022) proposed ReAct, which uses LLMs to generate reasoning traces and task-specific actions in an interleaved manner, thereby achieving greater synergy between the two. Additionally, recent works have used LLMs as components in building hierarchical modular decision-making agents, where they are only used to generate high-level plans and do not directly generate decisions (Ahn et al., 2022; Fu et al., 2023; Carta et al., 2023; Chen et al., 2024; Xu et al., 2024; Sha et al., 2023; Liu et al., 2023; Hu et al., 2024; Zhou et al., 2024). The VLA4CD model proposed here can be seen as a multimodal GPT model fine-tuned for a downstream application scenario, featured by its capability to simultaneously output action decisions and textual chatting.

## 2.2 VLA MODEL FOR DECISION-MAKING

The VLA model is a type of model designed to handle multimodal input of vision, language, and action to accomplish embodied decision-making tasks. Unlike traditional LLMs that are mostly used for constructing conversational AI represented by ChatGPT, VLA has the ability to generate a control signal for a physical entity, e.g., a Robot, that interacts with the environment. VLA has been widely used for instruction-following tasks, wherein it endows the agent with an ability to understand language instructions, visually perceive the environment, and generate appropriate actions (Huang et al., 2023; Li et al., 2023b; Zhen et al., 2024; Dorka et al.). Compared to deep reinforcement learning (RL) methods, VLA has shown a remarkable performance gain in versatility, flexibility, and generality in complex environments (Padalkar et al., 2023; Brohan et al., 2023; et al, 2024; Team et al., 2024; Li et al., 2023c; Bai et al., 2023; Li et al., 2022; 2023a; Liu et al., 2024; Tan & Bansal, 2019). However, such VLA models represented by RT-X (Padalkar et al., 2023) and OpenVLA (Kim et al., 2024), typically discretize continuous action spaces into fixed intervals. This action discretization raises significant limitations for them to deal with fine-grained continuous actions that are required for capturing nuanced operations necessary for some complex tasks. This issue is particularly pronounced in scenarios that require high precision and real-time responsiveness, such as autonomous driving.

In our VLA4CD, we propose a technique to avoid action discretization in VLA. In addition, we consider a new problem setting that differs from the instruction-following one. In our setting, the agent can chat with a human and make fine-grained decisions simultaneously. We found that if we directly use current VLA models into this setting, they perform unsatisfactorily as they tend to rely more on the text data to generate decisions while neglecting the critical role of visual information.

## 3 METHODOLOGY

In this section, we present how to build VLA4CD in detail, including the model architecture and the training procedure, with a focus on the loss designs in the last output hidden layer. An overview of VLA4CD is illustrated in Figure 1. To begin with, we present the problem setting of our concern.

### 3.1 PROBLEM SETTING

We consider a multimodal setting similar as (Xiao et al., 2020), wherein, at each time step  $t$ , upon the agent performs an action  $a_t$ , the environment returns an observation consisting of both visual and textual modalities, denoted by  $\{o_t, w_t\}$ . Our objective is to build a generative model  $\pi(a_t, \hat{w}_t | o_{t-H}, w_{t-H}, a_{t-H}, \dots, o_t, w_t)$ , which can generate both high-quality action decisions and text responses, given a sequence of historic observations and actions. Here,  $\hat{w}_t$  denotes a text-formed response to the text-formed input  $w_t$ . If  $w_t$  is a question, then  $\hat{w}_t$  can be seen as its answer given by our model.  $H$  denotes the length of the context.

### 3.2 MODEL ARCHITECTURE

Our model supports three different input modalities: text, image, and numeric vector. We use Llama-7b (Touvron et al., 2023b) as the backbone model, and encode textual inputs by its pre-trained

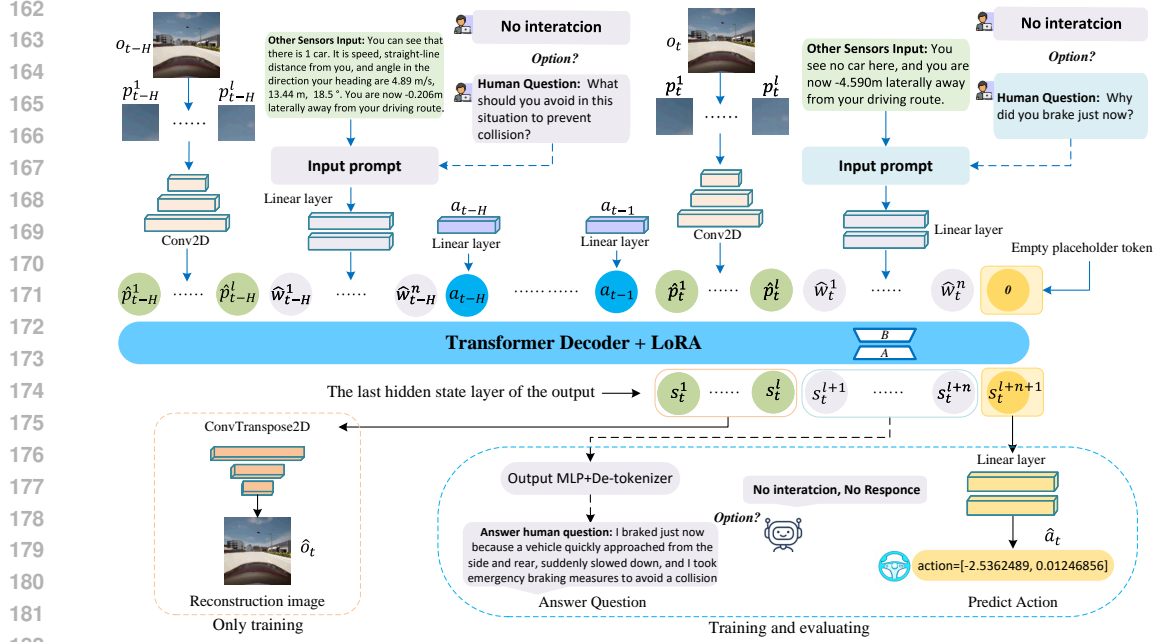


Figure 1: An overview of VLA4CD framework.

embedding layers. To encode the visual inputs, we follow the standard practice used in visual language models (VLMs) (Liu et al., 2024) and VLAs (Kim et al., 2024). Specifically, we first segment each input image  $o$  into  $L$  patches  $p_l$ ,  $l = 1, \dots, L$ , then train a 2D convolution network that directly maps the patches to the vector space. In addition, to deal with the input of the action value, we train a multi-layer perceptron (MLP) module that encodes the action values to the vector space. Finally, We concatenate encoded embeddings of all modalities together to form a sequence of embedded trajectory  $\tau$  at time  $t$  as follows:

$$\tau_t = \{(\hat{p}_{t-H}^1, \dots, \hat{p}_{t-H}^L), (\hat{w}_{t-H}^1, \dots, \hat{w}_{t-H}^n), a_{t-H}, \dots, (\hat{p}_t^1, \dots, \hat{p}_t^L), (\hat{w}_t^1, \dots, \hat{w}_t^n)\}, \quad (1)$$

where  $\hat{p}_t^i$  and  $\hat{w}_t^j$  denote the embeddings of  $i$ -th patch for visual observation and  $j$ -th token for textual observation at time  $t$ , respectively.

During the inference stage, the transformer backbone in VLA4CD generates the hidden embeddings  $s_t^{l+1}, \dots, s_t^{l+n+1}$  as shown in Figure 1, then these embeddings are decoded into the outputs of different modalities. Specifically, VLA4CD supports two different output modalities: text for chatting and numeric vector for action-level decision making. For the chatting part, we use the pre-trained output MLP layers and tokenizer of the Llama-7b model to generate texts. For action decision-making, our model generates one more embedding vector after the “< EOS >”, an empty placeholder token. Unlike previous work like OpenVLA (Kim et al., 2024) and RT-X (Brohan et al., 2023), in which action prediction is formalized as a token generation task by splitting the action space into discrete action bins, we train an action head consisting of a two-layer MLP module. This action head directly maps the output embedding to action values. We empirically find that using our approach leads to better performance compared to discretizing action values.

### 3.3 TRAINING PROCEDURE

We fine-tune the transformer backbone with LoRA (Hu et al., 2021) and train the image encoding module, text encoding module, action encoding, and decoding modules with an offline dataset  $D_{expert}$ , which contains demonstrated trajectories of driving vehicles with question-answer pairs related to this driving scenario. The training objective is to predict accurate actions for vehicle control and answer domain questions such as “Summarize the current driving scenario at a high level”. Moreover, to encourage the model to abstract key information from the images and prevent over-

fitting, we consider image reconstruction as an auxiliary task, adding a 2D transposed convolution layer to reconstruct input images patches from the output last hidden embeddings  $s_t^1, \dots, s_t^l$ , as illustrated in Figure 1. As a result, our training loss is composed of three items, corresponding to text generation, action prediction, and image reconstruction, respectively. Next, we describe each loss item in detail. For ease of presentation, we denote the parameters in the auxiliary image decoder as  $\phi$  and all other trainable parameters as  $\theta$ .

**Text Generation** In our experiment, we found that merely replacing specific numerical values in the translation template (Chen et al., 2024) results in minimal representational differences caused by the sequential nature of the data, making the phenomenon of model overfitting easy to happen if we use the conventional cross-entropy loss for text generation. Refer to Appendix A.7 for details. To mitigate this, we use the label smoothing technique to regularize the training process (Szegedy et al., 2016). Specifically, the hard label for token  $w_i$  is smoothed by assigning a small portion of the probability mass to incorrect classes:

$$q_i^k = \begin{cases} 1 - \epsilon & \text{if } k = y_i, \\ \frac{\epsilon}{K-1} & \text{otherwise,} \end{cases} \quad (2)$$

where  $\epsilon$  is the smoothing factor and  $K$  is the number of total classes, i.e., vocabulary size. That is to say, the loss item for text generation we finally use is:

$$\mathcal{L}_{\text{language}}(\theta) = \frac{1}{N} \sum_i \sum_k q_i^k \log p(k|\tau^{i-1}, \theta), \quad (3)$$

where  $\tau^{i-1}$  denotes the input token sequence before position  $i$ , used for predicting token  $i$ .  $N$  denotes the maximum padding length to unify the input text.

**Action Prediction** To directly predicts continuous action values instead of discrete action bins, we train our model with a mean square error (MSE) loss between the ground-truth action value  $a_t$  and the predicted value, as follows:

$$\mathcal{L}_{\text{action}}(\theta) = \frac{1}{T} \sum_t \frac{1}{D} \sum_d [(a_t^d - \pi(\tau_t, \theta))^2] \quad (4)$$

where  $D$  denotes the dimension of the action space. In our experiments, the action dimension is 2, corresponding to the acceleration and steering of the vehicle, respectively.

**Image Reconstruction** The visual modality data contains rich information about the states of the environment. However, we find that, with a limited dataset, directly training the image encoder from language and action losses is not sufficient, as it leads to information losses. Inspired by Hafner et al. (2019), we consider an auxiliary image reconstruction task to introduce additional supervision in the visual modality. Specifically, we use a 2D transposed convolution layer  $f_\phi$  to reconstruct each image patch from its corresponding output embedding and train the model to minimize the pixel-wise Euclidean distance between the original and reconstructed image patches:

$$\mathcal{L}_{\text{image}}(\theta, \phi) = \frac{1}{L} \sum_l \text{MSE}(o_t, f_\phi(\pi(g_\theta(\tau_t^{p_t^l}), \theta))), \quad (5)$$

where  $o_t$  is the input image, and  $\tau_t^{p_t^l}$  is the input sequence up to this patch token, and  $g_\theta$  represents a trainable 2D convolutional network that directly maps image patches  $p_t^1, \dots, p_t^l$  to the language embedding space  $\hat{p}_t^1, \dots, \hat{p}_t^l$ .

**Training Loss Function** In summary, our training loss function is defined as follows:

$$\mathcal{L}(\theta, \phi) = \alpha_1 \mathcal{L}_{\text{language}}(\theta) + \alpha_2 \mathcal{L}_{\text{action}}(\theta) + \lambda \mathcal{L}_{\text{image}}(\theta, \phi), \quad (6)$$

where  $\alpha_1, \alpha_2, \lambda$  are the weight hyperparameters of three components. In our experiments, we choose  $\alpha_1 = 0.1$ ,  $\alpha_2 = 10$ , and  $\lambda = 0.5$ .

## 4 EXPERIMENTS

In this section, we validate through experiments on the autonomous driving simulation platform CARLA that VLA4CD can make fine-grained action decisions while maintaining dialogue functionality. We also examine the impact of each loss term in our loss function design on the performance of



324  
325  
326  
327  
328  
329  
330  
331  
332  
333  
334  
335  
336  
337  
338  
339  
340  
341  
342  
343  
344  
345  
346  
347  
348  
349  
350  
351  
352  
353  
354  
355  
356  
357  
358  
359  
360  
361  
362  
363  
364  
365  
366  
367  
368  
369  
370  
371  
372  
373  
374  
375  
376  
377

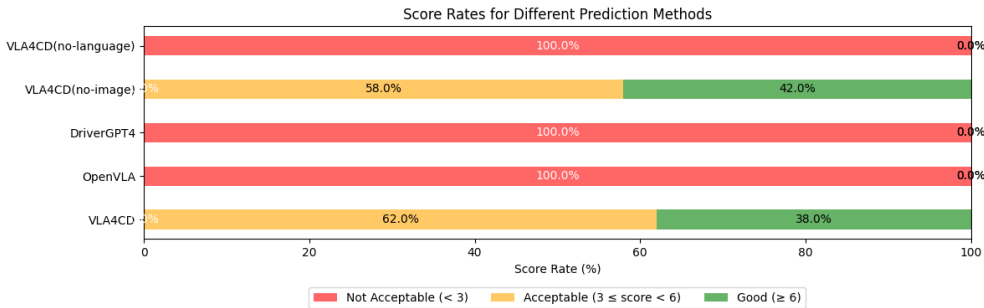


Figure 4: GPT-4o scores the answers from five methods for randomly generated inputs and question

of 1000 steps, with 200 involved vehicles, whose driving routes and met scenarios are generated in random mode.

The training dataset  $D_{expert}$  was obtained from the EGADS framework (Tang et al., 2024), which designs RL and imitation learning-based agent with safety constraints, demonstrating excellent performance in CARLA. Therefore, we select this agent as our experts. We let such experts drive vehicles in town03 of CARLA to collect the dataset. Town03 is one complex map in CARLA, closely resembling real urban road environments, including various complex scenarios such as tunnels, intersections, roundabouts, curves, and multi-turns, covering an area of 400m × 400m, with a total road length of approximately 6km. As shown in Figure 3 (b), we used the layout of the town03 map for training. In the experimental environment for data collection and online evaluation, all vehicles randomly select directions at intersections, follow randomly generated routes, slow down for preceding vehicles, and stop when the traffic light ahead turns red.

Following Chen et al. (2024), we design a template based parser that translates sensor data (such as position and distance information, excluding vision and lidar) into natural language descriptions, as shown in "other sensors input" in Figures 1 and 2. For details on the templates, refer to Appendix A.6. Note that such "other sensors input" does not include any action-related information from VLA4CD, such as speed and heading angle. In this way, we can test whether VLA4CD can leverage informative text data to enhance the quality of action decisions.

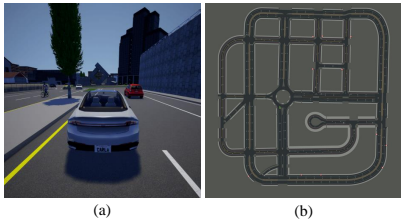


Figure 3: The (a) shows a sample view of the simulation environment, while the (b) presents a bird-eye view of our task scenario.

#### 4.4 PERFORMANCE METRICS

**Performance metrics for evaluating the chatting ability** We used the powerful model GPT-4o (OpenAI, 2023) to compare the quality of answers given by VLA4CD with baseline models. Specifically, we first chose 50 pieces of randomly generated environment information and questions in CARLA. Then, given a piece of environment information and a question, we let VLA4CD and a baseline model each generate an answer. Then we used GPT-4o to score them, with a maximum score of 10. The scoring criteria are as follows: Not Acceptable (< 3), Acceptable (3 ≤ score < 6), Good (≥ 6). Additionally, to assess the impact of the language and image components on dialogue capabilities, we included VLA4CD (no-language) and VLA4CD (no-image), two simplified versions of VLA4CD trained by removing the loss items corresponding to text generation and image reconstruction, respectively:  $\mathcal{L}_{action} + \mathcal{L}_{image}$ ,  $\mathcal{L}_{action} + \mathcal{L}_{language}$ .

**Performance metrics for evaluating the decision-making ability** We deployed our trained model on a car for use in navigating through a town. We considered commonly used metrics to evaluate the driving performance, including Collision Rate (CR), Off-road Rate (OR), Episode Completion Rate (ER), Average Safe Driving Distance (ASD), Average Reward (AR), and Driving Score (DS). DS is a composite indicator reflecting the overall performance of the vehicle in terms of safety, efficiency, and compliance with traffic rules. In addition, we use the reward function  $f$  as described

Table 1: Evaluation results for different methods in town03 (random),  $H=1$ 

Method	Input	DS $\uparrow$	AR ( $f$ ) $\uparrow$	ASD(m) $\uparrow$	ER(%) $\uparrow$	OR(%) $\downarrow$	CR(%) $\downarrow$
BC	image	20.21 $\pm$ 7.46	175.34 $\pm$ 72.86	54.21 $\pm$ 6.41	9.08 $\pm$ 0.56	54.86 $\pm$ 20.04	60.00 $\pm$ 11.23
DriverGPT4	image, text	-	-	-	-	-	-
Openvla	image, text	-13.02 $\pm$ 4.02	-199.16 $\pm$ 38.73	24.34 $\pm$ 5.02	5.25 $\pm$ 0.39	24.36 $\pm$ 4.17	95.00 $\pm$ 0.00
VLA4CD	image, text	92.78 $\pm$ 23.75	466.80 $\pm$ 91.66	71.77 $\pm$ 9.40	16.35 $\pm$ 1.56	15.33 $\pm$ 4.36	55.00 $\pm$ 11.41

Table 2: Evaluation results for different methods in town03 (random),  $H=4$ 

Method	Input	DS $\uparrow$	AR ( $f$ ) $\uparrow$	ASD(m) $\uparrow$	ER(%) $\uparrow$	OR(%) $\downarrow$	CR(%) $\downarrow$
BC	image	36.39 $\pm$ 13.37	314.66 $\pm$ 86.02	64.08 $\pm$ 10.48	9.04 $\pm$ 0.62	37.56 $\pm$ 16.44	45.00 $\pm$ 11.41
Dreamer	image	-0.03 $\pm$ 0.01	-14.96 $\pm$ 0.09	0.02 $\pm$ 0.01	0.22 $\pm$ 0.01	0.00 $\pm$ 0.00	0.00 $\pm$ 0.00
Forbes	image	0.98 $\pm$ 1.43	21.63 $\pm$ 21.72	22.84 $\pm$ 1.00	6.30 $\pm$ 0.31	18.78 $\pm$ 1.03	56.67 $\pm$ 9.20
DT	image	7.68 $\pm$ 3.24	51.97 $\pm$ 29.33	23.74 $\pm$ 2.47	9.92 $\pm$ 0.71	10.31 $\pm$ 2.32	65.00 $\pm$ 10.94
DriverGPT4	image, text	-	-	-	-	-	-
Openvla	image, text	-7.84 $\pm$ 0.67	-160.37 $\pm$ 7.85	18.03 $\pm$ 1.92	4.76 $\pm$ 0.19	20.77 $\pm$ 3.36	100.00 $\pm$ 0.00
VLA4CD	image, text	105.25 $\pm$ 14.03	349.52 $\pm$ 49.75	59.76 $\pm$ 5.04	25.02 $\pm$ 2.57	19.93 $\pm$ 2.11	30.00 $\pm$ 10.51

Table 3: Evaluation the generalization for different methods in town04 (random),  $H=4$ 

Method	Input	DS $\uparrow$	AR ( $f$ ) $\uparrow$	ASD(m) $\uparrow$	ER(%) $\uparrow$	OR(%) $\downarrow$	CR(%) $\downarrow$
BC	image	39.22 $\pm$ 11.64	358.79 $\pm$ 79.59	63.08 $\pm$ 9.37	8.69 $\pm$ 0.56	5.64 $\pm$ 1.26	60.00 $\pm$ 11.23
Dreamer	image	-0.03 $\pm$ 0.01	-15.03 $\pm$ 0.07	0.02 $\pm$ 0.01	0.01 $\pm$ 0.21	0.01 $\pm$ 0.00	0.00 $\pm$ 0.00
Forbes	image	-2.63 $\pm$ 2.75	-17.37 $\pm$ 22.98	19.79 $\pm$ 1.20	6.24 $\pm$ 0.69	15.80 $\pm$ 2.74	66.70 $\pm$ 8.75
DT	image	10.66 $\pm$ 3.26	85.58 $\pm$ 27.04	24.94 $\pm$ 2.92	10.55 $\pm$ 0.58	11.38 $\pm$ 2.15	55.00 $\pm$ 11.41
DriverGPT4	image, text	-	-	-	-	-	-
Openvla	image, text	-6.74 $\pm$ 0.88	-153.35 $\pm$ 10.26	13.62 $\pm$ 1.86	4.26 $\pm$ 0.17	15.70 $\pm$ 2.71	100.00 $\pm$ 0.00
VLA4CD	image, text	94.26 $\pm$ 15.26	384.52 $\pm$ 51.72	56.93 $\pm$ 4.03	21.49 $\pm$ 1.86	12.75 $\pm$ 2.28	45.00 $\pm$ 11.41

in Chen et al. (2019) in the AR metric for training RL baselines. This reward function scores yaw, collisions, speeding, and lateral velocity for ego vehicle. Finally, we selected the checkpoint with the highest DS and AR score. For details, refer to Appendix A.4 and Appendix A.5.

#### 4.5 EXPERIMENTAL RESULT ON CHATTING ABILITY EVALUATION

As shown in Figures 2 and 4, VLA4CD performs significantly better than others in terms of chatting ability. In contrast, OpenVLA performs poorly in question-answering because it focuses solely on optimizing the action loss. DriverGPT4 faces challenges as both tasks share the same decoder, causing the model to misinterpret inputs as only for action prediction, making it difficult to generate complete text. Despite having two independent loss items, the model has not effectively balanced these two losses. Furthermore, VLA4CD (no language) shows a significant gap in conversational ability compared to VLA4CD, while VLA4CD (no image) performs similarly to VLA4CD, highlighting the importance of the language loss component for enhancing chatting abilities.

#### 4.6 EXPERIMENTAL RESULT ON DECISION-MAKING ABILITY EVALUATION

We define the "-" in Tables 1, 2, and 3 as a failure standard if a complete action value is not generated within 50 seconds. As shown in Table 1, VLA4CD significantly outperforms BC and OpenVLA in terms of DS, AR, and ASD at a single time step, while DriverGPT4 fails to generate precise action values. VLA4CD also shows significant improvements over other methods across multiple time steps in Table 2, indicating sustained benefits over longer durations. We evaluated these models' generalization capability by training them on the town03 dataset and then evaluating them online in town04. As shown in Table 3, the primary metric DS of VLA4CD significantly exceeds that of the other methods, showcasing its strong generalization ability. Tables 1, 2, and 3 indicate that DriverGPT4 faces challenges in generating precise action values for real-time control commands, highlighting the difficulties of directly generating accurate values using a detokenizer. In contrast, OpenVLA can generate precise values in experiments but produces identical action commands, causing vehicles to wander or spin in a place, resulting in significant penalties. Results in Tables 2

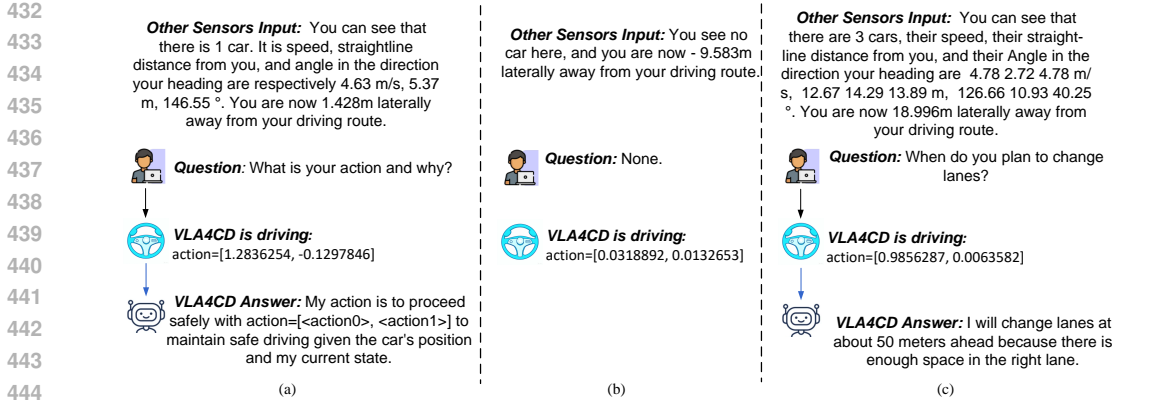


Figure 5: An example show on how VLA4CD smoothly engages in conversation with a human while simultaneously making real-time action decisions during the driving process

Table 4: Ablation studies on the loss function of VLA4CD in town03 (random),  $H=4$

Loss function	Input	DS $\uparrow$	AR ( $f$ ) $\uparrow$	ASD(m) $\uparrow$	ER(%) $\uparrow$	OR(%) $\downarrow$	CR(%) $\downarrow$
$\mathcal{L}_{\text{image}} + \mathcal{L}_{\text{language}} + \mathcal{L}_{\text{action-bins}}$	image, text	11.57 $\pm$ 0.00	142.83 $\pm$ 0.01	22.71 $\pm$ 0.01	8.10 $\pm$ 0.05	30.87 $\pm$ 0.10	100.00 $\pm$ 0.00
$\mathcal{L}_{\text{image}} + \mathcal{L}_{\text{action}}$	image, text	45.08 $\pm$ 10.88	234.36 $\pm$ 52.21	39.64 $\pm$ 4.03	14.13 $\pm$ 1.71	16.68 $\pm$ 3.15	30.00 $\pm$ 10.51
$\mathcal{L}_{\text{language}} + \mathcal{L}_{\text{action}}$	image, text	74.85 $\pm$ 10.97	331.78 $\pm$ 49.88	50.63 $\pm$ 4.73	18.62 $\pm$ 1.95	15.96 $\pm$ 2.45	25.00 $\pm$ 9.93
$\mathcal{L}_{\text{image}} + \mathcal{L}_{\text{language}} + \mathcal{L}_{\text{action}}$ (our)	image, text	105.25 $\pm$ 14.03	349.52 $\pm$ 49.75	59.76 $\pm$ 5.04	25.02 $\pm$ 2.57	19.93 $\pm$ 2.11	30.00 $\pm$ 10.51

and 3 demonstrated that VLA4CD also significantly outperforms DT, Dreamer, and Forbes in terms of decision-making and model generalization.

Finally, Figure 5 illustrates how our model smoothly engages in conversation with a human while simultaneously making real-time action decisions during the driving process.

#### 4.7 ABLATION STUDIES ON THE LOSS FUNCTION DESIGN

As shown in Equation (6), our loss function is composed of three losses, namely action loss  $\mathcal{L}_{\text{action}}$ , language loss  $\mathcal{L}_{\text{language}}$ , and image loss  $\mathcal{L}_{\text{image}}$ . We conducted ablation studies to investigate the effect of each loss on the performance of VLA4CD. The experiment result is shown in Table 4, where the action-bins loss  $\mathcal{L}_{\text{action-bins}}$  denotes the action loss used by OpenVLA and RT2. They deal with continuous valued actions by value discretization. We included VLA4CD (no-language) and VLA4CD (no-image), two simplified versions of VLA4CD trained by using  $\mathcal{L}_{\text{action}} + \mathcal{L}_{\text{image}}$  and  $\mathcal{L}_{\text{action}} + \mathcal{L}_{\text{language}}$ , respectively.

**On the effect of  $\mathcal{L}_{\text{action}}$**  As shown in Table 4, if we compare the performance metrics of  $\mathcal{L}_{\text{image}} + \mathcal{L}_{\text{language}} + \mathcal{L}_{\text{action-bins}}$  with that of  $\mathcal{L}_{\text{image}} + \mathcal{L}_{\text{language}} + \mathcal{L}_{\text{action}}$ , we can see a clear advantage of using our action loss  $\mathcal{L}_{\text{action}}$  over using  $\mathcal{L}_{\text{action-bins}}$ . This explains why VLA4CD outperforms VLA models that use the type of action loss similar to  $\mathcal{L}_{\text{action-bins}}$ , as shown in Tables 1, 2, and 3. Specifically, from our experiments, we found that doing action discretization and tokenization as in current VLA models lead to low training loss but bad inference performance. This is because adjacent action intervals are represented by consecutive token IDs (e.g., 31830 and 31831), which are close in token space. Consequently, the model tends to output the same token (31830 or 31831) in inference, while the actual action values corresponding to them can have significant differences. In contrast, our approach proposed to deal with continuously valued actions can avoid this phenomenon to happen.

**On the effect of  $\mathcal{L}_{\text{language}}$**  As shown in Table 4, if we compare performance metrics between  $\mathcal{L}_{\text{image}} + \mathcal{L}_{\text{action}}$  (corresponding to VLA4CD (no-language)) and  $\mathcal{L}_{\text{image}} + \mathcal{L}_{\text{language}} + \mathcal{L}_{\text{action}}$  (corresponding to VLA4CD), we see that including  $\mathcal{L}_{\text{language}}$  in the loss function significantly enhances the quality of decision-making. As shown in Figures 2 and 4, VLA4CD (no-language) has significantly different dialogue capabilities compared to VLA4CD, while VLA4CD (no-image) performs similarly to VLA4CD. It demonstrates that  $\mathcal{L}_{\text{language}}$  plays an important role for maintaining the dialogue

Table 5: The impact of the quality of textual modality data in training data on the decision-making performance of VLA4CD

Input	Noise ratio	DS $\uparrow$	AR ( $f$ ) $\uparrow$	ASD(m) $\uparrow$	ER(%) $\uparrow$	OR(%) $\downarrow$	CR(%) $\downarrow$
image, text	100%	-0.01 $\pm$ 1.12	-5.10 $\pm$ 0.00	0.00 $\pm$ 0.00	0.30 $\pm$ 0.00	0.00 $\pm$ 0.00	0.00 $\pm$ 0.00
image, text	75%	2.74 $\pm$ 2.17	16.93 $\pm$ 29.84	18.63 $\pm$ 1.70	7.38 $\pm$ 0.32	16.93 $\pm$ 2.32	55.0 $\pm$ 11.41
image, text	50%	4.41 $\pm$ 1.87	49.12 $\pm$ 12.56	6.10 $\pm$ 1.34	6.35 $\pm$ 0.67	0.00 $\pm$ 0.00	0.00 $\pm$ 0.00
image, text	25%	15.58 $\pm$ 2.49	143.70 $\pm$ 23.54	23.23 $\pm$ 3.24	8.25 $\pm$ 1.11	26.75 $\pm$ 1.83	10.00 $\pm$ 6.88
image, text	0%	93.89 $\pm$ 29.73	336.11 $\pm$ 86.72	45.42 $\pm$ 9.53	16.68 $\pm$ 2.50	19.05 $\pm$ 4.96	5.00 $\pm$ 5.00

capability. To summarize, including  $\mathcal{L}_{\text{language}}$  in the loss function has beneficial impacts on both dialogue and decision-making.

**On the effect of  $\mathcal{L}_{\text{image}}$**  As shown in Table 4, when we added  $\mathcal{L}_{\text{image}}$  in the loss function (corresponding to results of  $\mathcal{L}_{\text{image}} + \mathcal{L}_{\text{language}} + \mathcal{L}_{\text{action}}$ ), all performance metrics related to decision-making are increased in value, compared to  $\mathcal{L}_{\text{language}} + \mathcal{L}_{\text{action}}$ . This confirms that the  $\mathcal{L}_{\text{image}}$  indeed brings remarkable benefits for enhancing decision-making performance. We argue that this is because, during the decision-making, doing high-quality image reconstruction can further explore and utilize the rich information related to the current scene within the image modality data, thereby benefiting the decision-making.

#### 4.8 HOW THE QUALITY OF TEXTUAL MODALITY DATA IN TRAINING DATA AFFECTS THE DECISION-MAKING PERFORMANCE OF THE MODEL?

Imagine a driver is operating a car, with a friend sitting inside the vehicle and conversing with the driver. If this friend provides valuable reminders, such as alerting the driver to a car approaching from the blind spot, the friend’s words would be beneficial to the driver’s decision-making. On the contrary, if the friend’s words are irrelevant noise to the current situation, it might interfere with the driver’s ability to make accurate decisions. Therefore, we designed a set of experiments to test whether our model exhibits similar performance to that of human drivers in decision making. The result is presented in Table 5. As is shown, when we add more and more noisy information unrelated to driving scenarios into the text modality data in the training dataset, the quality of the decisions output by our model rapidly decreases. This indicates that the performance of our model is very similar to that of human drivers.

## 5 CONCLUSION

In this paper, we investigated how to develop a multimodal pre-trained model that simultaneously achieves the dialogue function of LLM and the decision-making function of VLA. We use the autonomous driving scenario as an example to explain our problem setup and model development process. Unlike the instruction-following setup used behind VLA models, our problem setup can be described as making decisions while conversing. In the former, text data appears in the form of instructions before the decision-making process; in the latter, text data and decision data are interwoven (imagine a large pre-trained model making driving decisions while chatting with people in the car). For the aforementioned problem setup, we provide a method for constructing a multimodal Visual Language Action model for simultaneously Chatting and Decision making (VLA4CD). Experimental results show that, thanks to our proposed way to deal with continuous valued actions, our design of the training cost function, and the use of label smoothing technique, our VLA4CD model significantly outperforms the SOTA VLA model, RL, and decision transformer methods in decision-making performance, while also possessing smooth dialogue capabilities.

VLA4CD can be seen as a functional extension of the VLA model, while its performance depends on the quality of the training data set. Interesting future research directions include: further testing and validation using large-scale real-world driving datasets; and applying our approach to scenarios beyond autonomous driving, such as home robots.

## REFERENCES

- 540  
541  
542 Michael Ahn, Yen-Ling Chen, Anthony Brohan, Mark McCarthy, Jonathan Carff, Matthew Hill,  
543 Jerry Tworek, Andrew Yuan, Michael Paster, Karol Hausman, et al. Do as i can, not as i say:  
544 Grounding language in robotic affordances. *arXiv preprint arXiv:2204.01691*, 2022.
- 545 Jinze Bai, Shuai Bai, Yunfei Chu, Zeyu Cui, Kai Dang, Xiaodong Deng, Yang Fan, Wenbin Ge,  
546 Yu Han, Fei Huang, et al. Qwen technical report. *arXiv preprint arXiv:2309.16609*, 2023.
- 547 Anthony Brohan, Noah Brown, Justice Carbajal, Yevgen Chebotar, Joseph Dabis, Chelsea Finn,  
548 Keerthana Gopalakrishnan, Karol Hausman, Alex Herzog, Jasmine Hsu, et al. Rt-1: Robotics  
549 transformer for real-world control at scale. *arXiv preprint arXiv:2212.06817*, 2022.
- 550 Anthony Brohan, Noah Brown, Justice Carbajal, Yevgen Chebotar, Xi Chen, Krzysztof Choroman-  
551 ski, Tianli Ding, Danny Driess, Avinava Dubey, Chelsea Finn, et al. Rt-2: Vision-language-action  
552 models transfer web knowledge to robotic control. *arXiv preprint arXiv:2307.15818*, 2023.
- 553 Tom Brown, Benjamin Mann, Nick Ryder, Melanie Subbiah, Jared Kaplan, Prafulla Dhariwal,  
554 Arvind Neelakantan, Pranav Shyam, Girish Sastry, Amanda Askell, et al. Language models are  
555 few-shot learners. *Advances in neural information processing systems*, 33:1877–1901, 2020.
- 556 Thomas Carta, Clément Romac, Thomas Wolf, Sylvain Lamprier, Olivier Sigaud, and Pierre-Yves  
557 Oudeyer. Grounding large language models in interactive environments with online reinforcement  
558 learning. In *International Conference on Machine Learning*, pp. 3676–3713. PMLR, 2023.
- 559 Jianyu Chen. An openai gym third party environment for carla simulator. <https://github.com/cjy1992/gym-carla?tab=readme-ov-file>, 2020.
- 560 Jianyu Chen, Bodi Yuan, and Masayoshi Tomizuka. Model-free deep reinforcement learning for  
561 urban autonomous driving. In *2019 IEEE intelligent transportation systems conference (ITSC)*,  
562 pp. 2765–2771. IEEE, 2019.
- 563 Lili Chen, Kevin Lu, Aravind Rajeswaran, Kimin Lee, Aditya Grover, Misha Laskin, Pieter Abbeel,  
564 Aravind Srinivas, and Igor Mordatch. Decision transformer: Reinforcement learning via sequence  
565 modeling. *Advances in neural information processing systems*, 34:15084–15097, 2021.
- 566 Long Chen, Oleg Sinavski, Jan Hünermann, Alice Karnsund, Andrew James Willmott, Danny Birch,  
567 Daniel Maund, and Jamie Shotton. Driving with llms: Fusing object-level vector modality for  
568 explainable autonomous driving. In *2024 IEEE International Conference on Robotics and Au-*  
569 *tomation (ICRA)*, pp. 14093–14100. IEEE, 2024.
- 570 Xiaoyu Chen, Yao Mark Mu, Ping Luo, Shengbo Li, and Jianyu Chen. Flow-based recurrent belief  
571 state learning for pomdps. In *International Conference on Machine Learning*, pp. 3444–3468.  
572 PMLR, 2022.
- 573 Nicolai Dorka, Chenguang Huang, Tim Welschhold, and Wolfram Burgard. What matters in em-  
574 ploying vision language models for tokenizing actions in robot control? In *First Workshop on*  
575 *Vision-Language Models for Navigation and Manipulation at ICRA 2024*.
- 576 Alexey Dosovitskiy, German Ros, Felipe Codevilla, Antonio Lopez, and Vladlen Koltun. Carla: An  
577 open urban driving simulator. In *Conference on robot learning*, pp. 1–16. PMLR, 2017.
- 578 A. S. et al. Introducing rfm-1: Giving robots human-like reasoning capabilities.  
579 *Introducingrfm-1:Givingrobotshuman-likereasoningcapabilities*, 2024.
- 580 Justin Fu, Kelvin Zhang, Utkarsh Sanyal, Lantao Yu, Collin Moses, Fan Yang, Stefano Ermon, and  
581 Zhibin Zhao. Driving with reasoning: Reinforcement learning with generalist language models  
582 for interpretable policies. *arXiv preprint arXiv:2303.00745*, 2023.
- 583 Danijar Hafner, Timothy Lillicrap, Jimmy Ba, and Mohammad Norouzi. Dream to control: Learning  
584 behaviors by latent imagination. *arXiv preprint arXiv:1912.01603*, 2019.
- 585 Bin Hu, Chenyang Zhao, Pu Zhang, Zihao Zhou, Yuanhang Yang, Zenglin Xu, and Bin Liu. En-  
586 abling intelligent interactions between an agent and an llm: A reinforcement learning approach.  
587 *Reinforcement Learning Conference (RLC)*, 2024.
- 588  
589  
590  
591  
592  
593

- 594 Edward J Hu, Yelong Shen, Phillip Wallis, Zeyuan Allen-Zhu, Yuanzhi Li, Shean Wang, Lu Wang,  
595 and Weizhu Chen. Lora: Low-rank adaptation of large language models. *arXiv preprint*  
596 *arXiv:2106.09685*, 2021.
- 597
- 598 Jiangyong Huang, Silong Yong, Xiaojian Ma, Xiongkun Linghu, Puhao Li, Yan Wang, Qing Li,  
599 Song-Chun Zhu, Baoxiong Jia, and Siyuan Huang. An embodied generalist agent in 3d world.  
600 *arXiv preprint arXiv:2311.12871*, 2023.
- 601 Chia-Chun Hung, Timothy Lillicrap, Josh Abramson, Yan Wu, Mehdi Mirza, Federico Carnevale,  
602 Arun Ahuja, and Greg Wayne. Optimizing agent behavior over long time scales by transporting  
603 value. *Nature communications*, 10(1):5223, 2019.
- 604
- 605 Moo Jin Kim, Karl Pertsch, Siddharth Karamcheti, Ted Xiao, Ashwin Balakrishna, Suraj Nair,  
606 Rafael Rafailov, Ethan Foster, Grace Lam, Pannag Sanketi, et al. Openvla: An open-source  
607 vision-language-action model. *arXiv preprint arXiv:2406.09246*, 2024.
- 608 Junnan Li, Dongxu Li, Caiming Xiong, and Steven Hoi. Blip: Bootstrapping language-image pre-  
609 training for unified vision-language understanding and generation. In *International conference on*  
610 *machine learning*, pp. 12888–12900. PMLR, 2022.
- 611 Junnan Li, Dongxu Li, Silvio Savarese, and Steven Hoi. Blip-2: Bootstrapping language-image  
612 pre-training with frozen image encoders and large language models. In *International conference*  
613 *on machine learning*, pp. 19730–19742. PMLR, 2023a.
- 614
- 615 Xinghang Li, Minghuan Liu, Hanbo Zhang, Cunjun Yu, Jie Xu, Hongtao Wu, Chilam Cheang,  
616 Ya Jing, Weinan Zhang, Huaping Liu, et al. Vision-language foundation models as effective robot  
617 imitators. *arXiv preprint arXiv:2311.01378*, 2023b.
- 618 Yuanzhi Li, Sébastien Bubeck, Ronen Eldan, Allie Del Giorno, Suriya Gunasekar, and Yin Tat Lee.  
619 Textbooks are all you need ii: phi-1.5 technical report. *arXiv preprint arXiv:2309.05463*, 2023c.
- 620
- 621 Haotian Liu, Chunyuan Li, Qingyang Wu, and Yong Jae Lee. Visual instruction tuning. *Advances*  
622 *in neural information processing systems*, 36, 2024.
- 623
- 624 Jiaqi Liu, Peng Hang, Xiao Qi, Jianqiang Wang, and Jian Sun. Mtd-gpt: A multi-task decision-  
625 making gpt model for autonomous driving at unsignalized intersections. In *2023 IEEE 26th*  
626 *International Conference on Intelligent Transportation Systems (ITSC)*, pp. 5154–5161. IEEE,  
627 2023.
- 628 OpenAI. Gpt-4 technical report, 2023. URL <https://openai.com/research/gpt-4>.
- 629
- 630 Abhishek Padalkar, Acorn Pooley, Ajinkya Jain, Alex Bewley, Alex Herzog, Alex Irpan, Alexander  
631 Khazatsky, Anant Rai, Anikait Singh, Anthony Brohan, et al. Open x-embodiment: Robotic  
632 learning datasets and rt-x models. *arXiv preprint arXiv:2310.08864*, 2023.
- 633 Hao Sha, Yao Mu, Yuxuan Jiang, Li Chen, Chenfeng Xu, Ping Luo, Shengbo Eben Li, Masayoshi  
634 Tomizuka, Wei Zhan, and Mingyu Ding. Languagempc: Large language models as decision  
635 makers for autonomous driving. *arXiv preprint arXiv:2310.03026*, 2023.
- 636
- 637 Christian Szegedy, Vincent Vanhoucke, Sergey Ioffe, Jon Shlens, and Zbigniew Wojna. Rethink-  
638 ing the inception architecture for computer vision. In *Proceedings of the IEEE conference on*  
639 *computer vision and pattern recognition*, pp. 2818–2826, 2016.
- 640 Hao Tan and Mohit Bansal. Lxmert: Learning cross-modality encoder representations from trans-  
641 formers. *arXiv preprint arXiv:1908.07490*, 2019.
- 642
- 643 Zuojin Tang, Xiaoyu Chen, YongQiang Li, and Jianyu Chen. Safe and generalized end-to-end  
644 autonomous driving system with reinforcement learning and demonstrations. *arXiv preprint*  
645 *arXiv:2401.11792*, 2024.
- 646 Gemma Team, Thomas Mesnard, Cassidy Hardin, Robert Dadashi, Surya Bhupatiraju, Shreya  
647 Pathak, Laurent Sifre, Morgane Rivière, Mihir Sanjay Kale, Juliette Love, et al. Gemma: Open  
models based on gemini research and technology. *arXiv preprint arXiv:2403.08295*, 2024.

648 Hugo Touvron, Thibaut Lavril, Gautier Izacard, Xavier Martinet, Marie-Anne Lachaux, Timothée  
649 Lacroix, Baptiste Rozière, Naman Goyal, Eric Hambro, Faysal Azhar, et al. Llama: Open and  
650 efficient foundation language models. *arXiv preprint arXiv:2302.13971*, 2023a.  
651

652 Hugo Touvron, Louis Martin, Kevin Stone, Pierre-Emmanuel Albert, Amjad Almahairi, Yasmine  
653 Babaei, Dmytro Bashlykov, Subhojit Batra, Anurag Bhargava, Shruti Bhosale, et al. Llama 2:  
654 Open foundation and fine-tuned chat models. *arXiv preprint arXiv:2307.09288*, 2023b.

655 Jason Wei, Xuezhi Wang, Dale Schuurmans, Maarten Bosma, Fei Xia, Ed Chi, Quoc V Le, Denny  
656 Zhou, et al. Chain-of-thought prompting elicits reasoning in large language models. *Advances in  
657 neural information processing systems*, 35:24824–24837, 2022.  
658

659 Yi Xiao, Felipe Codevilla, Akhil Gurrarn, Onay Urfalioglu, and Antonio M López. Multimodal  
660 end-to-end autonomous driving. *IEEE Transactions on Intelligent Transportation Systems*, 23(1):  
661 537–547, 2020.

662 Zhenhua Xu, Yujia Zhang, Enze Xie, Zhen Zhao, Yong Guo, Kwan-Yee K Wong, Zhenguo Li, and  
663 Hengshuang Zhao. Drivegpt4: Interpretable end-to-end autonomous driving via large language  
664 model. *IEEE Robotics and Automation Letters*, 2024.

665 Shunyu Yao, Jeffrey Wu, Daisy Zhe Liu, Dale Schuurmans, Quoc V Le, Denny Zhou, Yuan Cao,  
666 and Andrew Dai. React: Synergizing reasoning and acting in language models. *arXiv preprint  
667 arXiv:2210.03629*, 2022.  
668

669 Haoyu Zhen, Xiaowen Qiu, Peihao Chen, Jincheng Yang, Xin Yan, Yilun Du, Yining Hong, and  
670 Chuang Gan. 3d-vla: A 3d vision-language-action generative world model. *arXiv preprint  
671 arXiv:2403.09631*, 2024.

672 Zihao Zhou, Bin Hu, Pu Zhang, Chenyang Zhao, and Bin Liu. Large language model as a policy  
673 teacher for training reinforcement learning agents. *International Joint Conference on Artificial  
674 Intelligence (IJCAI)*, 2024.  
675  
676  
677  
678  
679  
680  
681  
682  
683  
684  
685  
686  
687  
688  
689  
690  
691  
692  
693  
694  
695  
696  
697  
698  
699  
700  
701

## A APPENDIX

### A.1 HYPERPARAMETER SETTINGS

In this section, we respectively introduce the model parameters of VLM4EDM, the parameters of the custom linear layers, as well as the parameters of gym-carla and evaluation, as shown in Tables 6, 7, and 8.

Table 6: Hyperparameters

Parameter	Value
batch_size	64
micro_batch_size	8
num_epochs	3
learning_rate	3e-4
cutoff_len	424
val_set_size	0.1
save_step	25
lora_r	8
lora_alpha	16
lora_dropout	0.05
lora_target_modules	{q_proj, k_proj}
Other Sensors Input_types	{obs, text}
lambda_action	10
lambda_smooth	0.1
lambda_img	0.5
horizon	1
regular_action_loss	False
img_patch_size	16

Table 7: Model Parameters and Layers

Parameter/Layer	Details
num_patches	64
tokenizer_vocab_size	32000
split_obs_proj	Conv2d(3, 4096, kernel_size=16, stride=16)
inverse_split_obs_proj	ConvTranspose2d(4096, 3, kernel_size=16, stride=16)
split_obs_position_embedding	Parameter(torch.randn(1, 64, 4096))
text_embedding	nn.Embedding(32000, 4096)
custom_lm_head	Linear(4096, 32000, bias=False)
actor_linear1	Linear(4096, 2048)
actor_linear2	Linear(2048, 1024)
actor_linear3	Linear(1024, 512)
actor_linear4	Linear(512, 256)
actor_linear5	Linear(256, 128)
actor_linear6	Linear(128, 64)
actor_linear7	Linear(64, 2)
reconstruction_layer	Linear(4096, micro_batch_size*3*128*128)
action_linear	Linear(2, 4096)

### A.2 CARLA MAPS

In order to comprehensively evaluate the performance of our EGADS, we utilized five maps in CARLA, including town03, town04 as shown in Figure 6. Town03 is a larger town with features of a downtown urban area. The map includes some interesting road network features such as a

756  
757  
758  
759  
760  
761  
762  
763  
764  
765  
766  
767  
768  
769  
770  
771  
772  
773  
774  
775  
776  
777  
778  
779  
780  
781  
782  
783

Table 8: gym-carla and evaluation Environment Parameters

Parameter	Value
Number of Vehicles	200
Number of Walkers	0
Random Seed	1
Other Sensors Input_names	lidar_noground
Display Size	400
Max Past Step	1
Time Step (dt)	0.1
Discrete Control	False
Continuous Acceleration Range	[-3.0, 3.0]
Continuous Steering Range	[-0.2, 0.2]
Ego Vehicle Filter	vehicle.lincoln*
Traffic Manager Port	Random integer (2000 to 9000)
Town Map	town03 or town04
Task Mode	Random
Max Time per Episode	2000
Max Waypoints	12
Observation Range	32
LiDAR Bin Size	0.25
Distance Behind Ego Vehicle	12
Lane Threshold	2.0
Desired Speed	8
Max Ego Vehicle Spawn Times	200
Display Route	True
PIXOR Grid Size	64
PIXOR Mode	False
Predict Speed	True

784  
785  
786  
787  
788  
789  
790  
791  
792  
793



794  
795  
796  
797  
798  
799

Figure 6: CARLA maps

800  
801  
802

roundabout, underpasses and overpasses. The town also includes a raised metro track and a large building under construction. Town04 is a small town with a backdrop of snow-capped mountains and conifers. A multi-lane road circumnavigates the town in a "figure of 8".

803  
804  
805

### A.3 IS MODEL DECISION-MAKING ABILITY ENHANCED WITH LONGER CONTEXT OF TRAJECTORIES?

806  
807  
808  
809

As shown in Table 9, we observed that although the context length  $H$  of input trajectories is longer, the overall DS and AR of VLA4CD show some improvement, but the increase is not significant. This improvement is primarily attributed to the higher route completion and lower collision rates associated with longer time steps. According to Section 4.3, when  $H = 4$ , the sequence length

Table 9: Evaluation VLA4CD longer context results for multmodal input in town03 (random)

Input	$\mathcal{L}_{\text{image}}$	$H$	DS $\uparrow$	AR ( $f$ ) $\uparrow$	ASD(m) $\uparrow$	ER(%) $\uparrow$	OR(%) $\downarrow$	CR(%) $\downarrow$
image	$\times$	1	29.55 $\pm$ 6.17	226.91 $\pm$ 42.24	54.24 $\pm$ 4.30	11.85 $\pm$ 0.68	20.22 $\pm$ 5.57	70.00 $\pm$ 10.5
image	$\times$	4	22.38 $\pm$ 4.96	155.79 $\pm$ 31.87	32.45 $\pm$ 1.74	14.41 $\pm$ 0.59	15.93 $\pm$ 2.65	40.00 $\pm$ 11.23
text	$\times$	1	37.44 $\pm$ 10.11	248.89 $\pm$ 52.91	47.37 $\pm$ 5.43	15.63 $\pm$ 1.98	17.02 $\pm$ 2.71	40.00 $\pm$ 11.24
text	$\times$	4	44.16 $\pm$ 7.39	252.10 $\pm$ 38.94	46.96 $\pm$ 3.23	15.66 $\pm$ 1.06	12.86 $\pm$ 2.45	60.00 $\pm$ 11.23
image, text	$\times$	1	68.10 $\pm$ 13.20	417.24 $\pm$ 57.41	58.81 $\pm$ 6.55	13.71 $\pm$ 1.26	11.39 $\pm$ 2.41	40.00 $\pm$ 11.24
image, text	$\times$	4	74.85 $\pm$ 10.97	331.78 $\pm$ 49.88	50.63 $\pm$ 4.73	18.62 $\pm$ 1.95	15.96 $\pm$ 2.45	25.00 $\pm$ 9.93
image, text	$\checkmark$	1	92.78 $\pm$ 23.75	466.80 $\pm$ 91.66	71.77 $\pm$ 9.40	16.35 $\pm$ 1.56	15.33 $\pm$ 4.36	55.00 $\pm$ 11.41
image, text	$\checkmark$	4	105.25 $\pm$ 14.03	349.52 $\pm$ 49.75	59.76 $\pm$ 5.04	25.02 $\pm$ 2.57	19.93 $\pm$ 2.11	30.00 $\pm$ 10.51

extends to 1956, representing a fourfold increase in sequence length. Despite this, the improvement in DS and AR scores is not pronounced. Notably, in metrics such as AR and ADS, the performance of  $H = 4$  is even worse than that of  $H = 1$ . This suggests that the input information might be redundant, and excessively long trajectories could negatively impact decision-making ability.

This result highlights several key issues. First, while longer context lengths provide the model with more historical context and information, an excessive amount of information may hinder the ability of model to effectively filter and extract useful decision signals, leading to information redundancy. Redundant information not only increases the computational complexity but also may distract the attention of model, reducing its capacity to capture critical features and thereby affecting overall decision-making. Therefore, shorter context length sequences provide more concise and precise inputs, facilitating quicker and more accurate judgments by the model. This indicates that the current fusion method has limited performance improvements. Chen et al. (2021); Hung et al. (2019) suggest that longer context lengths can bring more benefits for decision control, so we also consider how to compress historical information and efficiently fuse it in the future to enhance decision-making.

#### A.4 REWARD FUNCTION

We use the default reward function of the Gym-Carla benchmark (Chen, 2020) to evaluate all experimental methods, as follows:

$$f = 200r_c + v_{lon} + 10r_f + r_o - 5\alpha^2 + 0.2r_{lat} - 0.1 \quad (7)$$

where  $r_c$  is the reward related to collision, which is set to -1 if the ego vehicle collides and 0 otherwise.  $v_{lon}$  is the longitudinal speed of the ego vehicle.  $r_f$  is the reward related to running too fast, which is set to  $-1$  if it exceeds the desired speed (8 m/s here) and 0 otherwise.  $r_o$  is set to  $-1$  if the ego vehicle runs out of the lane, and 0 otherwise.  $\alpha$  is the steering angle of the ego vehicle in radians.  $r_{lat}$  is the reward related to lateral acceleration, which is calculated by  $r_{lat} = -|\alpha| \cdot v_{lon}^2$ . The last constant term is added to prevent the ego vehicle from standing still.

#### A.5 MEASURE PERFORMANCE METRICS

We use multiple key metrics to evaluate the performance of autonomous driving models in various driving scenarios. Collision Rate (CR): the frequency at which the vehicle collides with obstacles or other vehicles. This metric is critical for assessing the safety of the driving model. Outlane Rate (OR): the rate at which the vehicle deviates from its designated lane. This metric evaluates the ability of modes to maintain proper lane discipline. Episode Completion Rate (ER): the percentage of driving tasks or episodes that the vehicle successfully completes. Higher completion rates indicate better task performance. Average Safe Driving Distance (ASD): the average distance driven without incidents, such as collisions or off-road events. This metric highlights the capability to drive safely over extended periods. Average Return (AR): A metric that measures the cumulative reward collected by the vehicle during its driving tasks, often reflecting both task performance and adherence to safety guidelines. Driving Score (DS): A comprehensive metric that reflects the overall performance of the vehicle in terms of safety, efficiency, and compliance with traffic rules.

$$CR = \frac{N_{\text{collisions}}}{N_{\text{total.episodes}}}, OR = \frac{N_{\text{off\_road\_events}}}{N_{\text{total.episodes}}}, ER = \frac{N_{\text{completed\_steps}}}{N_{\text{total.steps}}} \quad (8)$$

$$ASD = \frac{\sum_{i=1}^{N_{\text{episodes}}} \text{distance}_i}{N_{\text{total\_episodes}}}, DS = ER \times AR \quad (9)$$

Where  $N_{\text{collisions}}$  is the number of collisions during the episode, and  $N_{\text{total\_episodes}}$  is the total number of episodes in the test. Where  $N_{\text{off\_road\_events}}$  is the number of times the vehicle went off-road, and  $N_{\text{total\_steps}}$  is the total number of episodes. Where  $\text{distance}_i$  is the distance driven during the  $i$ -th safe driving episode, and  $N_{\text{safe\_episodes}}$  is the number of episodes without incidents (such as collisions or off-road events). Where  $N_{\text{completed\_steps}}$  is the number of successfully completed steps, and  $N_{\text{total\_steps}}$  is the total number of steps in the episode. Where  $AR$  is the average reward  $f$  collected during the episode.

#### A.6 THE NATURAL LANGUAGE TEMPLATE FOR TEXT INPUT

We obtained information from the CARLA environment using other sensors (such as speed sensors and position sensors), excluding the acceleration and steering (action) of the ego vehicle). This information is transformed into a natural language template that the VLA can understand, as shown below:

```
<lateral_dis, delta_yaw, speed, vehicles_info> = <observation_vehicle_state>
<vehicles_num> = <len(vehicles_info)>
<multi_dis += str(vehicles_info[i][0])+"" , multi_yaw += str(vehicles_info[i][1])+"" , multi_speed
+= str(vehicles_info[i][2])+"">
<if vehicles_num=1:>
<new_input="You can see that there is a car. It is speed, straight-line distance from you, and angle
in the direction your heading are respectively {multi_speed} m/s, {multi_dis} m, {multi_yaw}°."
"You are now {lateral_dis}m laterally away from your driving route. ">
<elif vehicles_num>1:>
<new_input="You can see that there are vehicles_num cars. Their speed, straight-line distance
from you, and angle in the direction your heading are respectively {multi_speed} m/s, {multi_dis}
m, {multi_yaw}°." "You are now {lateral_dis}m laterally away from your driving route. ">
<elif vehicles_num=0:>
<new_input="You see no car here, and you are now {lateral_dis}m laterally away from your
driving route.">
```

#### A.7 THE BENEFITS OF CROSS-ENTROPY LOSS AND LABEL SMOOTHING LOSS FOR VLA4CD

We found that merely replacing specific numerical values in the translation template (Chen et al., 2024) results in minimal representational differences caused by the sequential nature of data, making it easy for conventional cross-entropy loss to lead to overfitting in text generation tasks. As shown in Table 10, we tested on both town03 and town04, which led to a decline in the decision-making performance of model. Compared to cross-entropy loss, cross-entropy loss with smoothed labels performed better. Therefore, we chose cross-entropy loss with smoothed labels as the loss for text generation in VLA4CD in our experiments.

#### A.8 THE IMPACT OF TRAINING DATA-RELATED FACTORS ON THE DECISION PERFORMANCE OF MODEL

In the multimodal ablation experiments on the VLA4CD model, as shown in Table 11, we systematically removed or replaced individual modalities to evaluate their contribution to decision-making. The results show that models utilizing image and text fusion significantly outperform those with only a single image or text input in terms of decision accuracy and stability. This indicates that the text modality in our dataset provides higher-level semantic abstraction to complement visual inputs, thereby enhancing overall decision-making ability. In addition, as shown in Table 11, a single text input performs better than a single image input, indicating that the information provided by the text modality in our dataset (especially from "other sensors input", as shown in Figure 2) is highly beneficial for improving the decision-making ability of model.

Table 10: We evaluated the performance of VLA4CD using smooth label loss and cross-entropy loss functions,  $H=4$ 

$\mathcal{L}_{\text{language}}$	Town	DS $\uparrow$	AR ( $f$ ) $\uparrow$	ASD(m) $\uparrow$	ER(%) $\uparrow$	OR(%) $\downarrow$	CR(%) $\downarrow$
Cross Entropy	town03	48.97 $\pm$ 7.60	296.53 $\pm$ 40.72	47.10 $\pm$ 4.87	15.37 $\pm$ 0.85	12.41 $\pm$ 2.73	35.00 $\pm$ 10.94
Smooth Label	town03	105.25 $\pm$ 14.03	349.52 $\pm$ 49.75	59.76 $\pm$ 5.04	25.02 $\pm$ 2.57	19.93 $\pm$ 2.11	30.00 $\pm$ 10.51
Cross Entropy	town04	66.69 $\pm$ 16.97	358.11 $\pm$ 61.10	52.72 $\pm$ 5.44	15.43 $\pm$ 1.11	9.63 $\pm$ 1.42	55.00 $\pm$ 11.41
Smooth Label	town04	94.26 $\pm$ 15.26	384.52 $\pm$ 51.72	56.93 $\pm$ 4.03	21.49 $\pm$ 1.86	12.75 $\pm$ 2.28	45.00 $\pm$ 11.41

Table 11: Evaluating the impact of different modal inputs on the decision-making of VLA4CD in town03 (random),  $H=4$ 

Input	$\mathcal{L}_{\text{image}}$	DS $\uparrow$	AR ( $f$ ) $\uparrow$	ASD(m) $\uparrow$	ER(%) $\uparrow$	OR(%) $\downarrow$	CR(%) $\downarrow$
image	$\times$	22.38 $\pm$ 4.96	155.79 $\pm$ 31.87	32.45 $\pm$ 1.74	14.41 $\pm$ 0.59	15.93 $\pm$ 2.65	40.00 $\pm$ 11.23
text	$\times$	44.16 $\pm$ 7.39	252.10 $\pm$ 38.94	46.96 $\pm$ 3.23	15.66 $\pm$ 1.06	12.86 $\pm$ 2.45	60.00 $\pm$ 11.23
image, text	$\times$	74.85 $\pm$ 10.97	331.78 $\pm$ 49.88	50.63 $\pm$ 4.73	18.62 $\pm$ 1.95	15.96 $\pm$ 2.45	25.00 $\pm$ 9.93
image, text	$\checkmark$	105.25 $\pm$ 14.03	349.52 $\pm$ 49.75	59.76 $\pm$ 5.04	25.02 $\pm$ 2.57	19.93 $\pm$ 2.11	30.00 $\pm$ 10.51

## A.9 THE NOISE CONSISTED OF INFORMATION DATASETS

The noise consisted of information completely unrelated to the current driving scenario as follow: {"A playful puppy brings joy and laughter to our days", "The whisper of the wind carries secrets of the universe", "A hidden garden blooms with the magic of nature's colors", "The aroma of fresh coffee awakens the senses each morning", "A handwritten letter feels like a warm hug from afar", "The glimmer of fireflies creates a magical summer night", "A spontaneous adventure can lead to unforgettable memories", "The serenity of a quiet lake reflects the beauty of the world", "A gentle touch can convey love without a single word", "The laughter of friends is the sweetest melody of all", "A warm hug is a universal language of comfort", "The dance of leaves in the breeze tells stories of change", "A cozy fire invites stories and shared moments", "The beauty of art inspires creativity and self-expression", "A day spent volunteering fills the heart with purpose", "The excitement of a new book is like embarking on a journey", "A delicious meal shared brings people closer together", "The sound of laughter can brighten even the gloomiest day", "A fleeting moment can hold the weight of a thousand memories", "The charm of small towns lies in their simple beauty", "A gentle rain nurtures the earth and inspires growth", "A colorful painting captures the essence of joy", "The peace of a mountain retreat refreshes the soul", "A favorite mug holds warmth and comfort on a chilly day", "The rustle of leaves underfoot reminds us of nature's rhythm", "A well-crafted story has the power to transport us anywhere", "The thrill of discovery keeps our spirits young and curious", "A cherished photograph holds a lifetime of memories", "The beauty of winter blankets the world in quiet calm", "A moment of kindness can change the trajectory of a day", "The aroma of spices fills the kitchen with warmth and love", "A shared joke creates bonds that laughter alone cannot", "The glow of a sunrise fills the heart with hope", "A melody can linger in the mind long after it fades", "The colors of autumn leaves create a vibrant tapestry", "A soft pillow cradles the head and invites sweet dreams", "The laughter of children brings joy and light to our lives", "A surprise visit from a friend can brighten any day", "The beauty of a flower garden is a celebration of life", "A good book can be a loyal companion on lonely nights", "The embrace of nature can heal and rejuvenate the spirit", "A treasure hunt ignites the spirit of adventure", "The warmth of homemade cookies fills the home with love", "A playful kitten brings joy and mischief to our lives", "The scent of pine trees evokes memories of the forest", }

## A.10 OUR DEFINED SET OF PROBLEMS

Randomly selected a question from the set of questions. = {"What are you seeing/observing?", "What are you paying attention to and why?", "Are there any traffic lights? What's the color of the traffic light?", "What's your current speed and steering angle?", "What is your action and why?", "Summarize the current driving scenario at a high level.", "How are you going to drive in this situation and why?", "What's the straight-line distance to the nearest car?", "What is the angle of the nearest car relative to your heading?", "Is there any lateral deviation from your driving route?", "What should be your next steering action?", "What should be your next acceleration command?", "Is there any moving object around you?", "Describe the position of the car relative to your head-







